UNIVERSITETET I OSLO
UNIVERSITY OF OSLO

Choice of single-particle potential and the convergence of the effective interaction.

M.Hjorth-Jensen, E. Osnes
Department of Physics, University of Oslo,
Box 1048 Blindern, 0316 Oslo 3, Norway

H. MUther and K.W. Schmid
Institut fUr Theoretische Physik
Universität TUbingen, Auf der Morgenstelle 14,
D-7400 TUbingen, Fed.Rep. Germany

Report 90-05 Received: 1990-02-22
ISSN-0332-5571

FYSISK INSTITUTT
DEPARTMENT OF PHYSICS

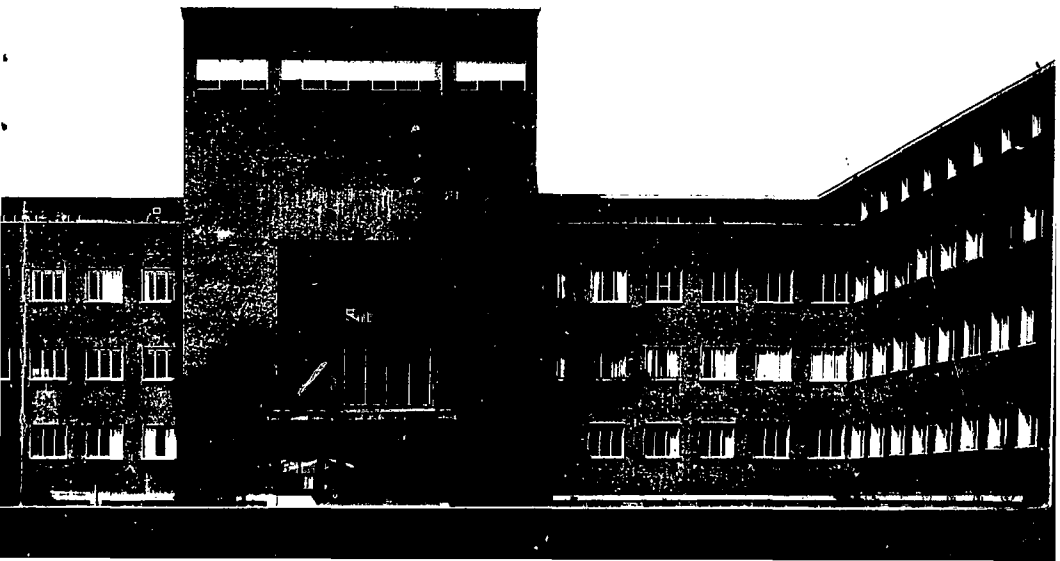

Choice of single-particle potential and the convergence of the effective interaction.

M.Hjorth-Jensen, E. Osnes
Department of Physics, University of Oslo,
Box 1048 Blindern, 0316 Oslo 3, Norway

H. MUther and K.W. Schmid
Institut fUr Theoretische Physik
Universität TUbingen, Auf der Morgenstelle 14,
D-7400 TUbingen, Fed.Rep. Germany

Report 90-05 Received: 1990-02-22
ISSN-0332-5571

Choice of single-particle potential and the convergence of the effective interaction.

M. Hjorth-Jensen, E. Osnes
Department of Physics, University of Oslo,
Box 1048 Blindern, N-0316 Oslo 3, Norway

H. Müther and K.W. Schmid
Institut für Theoretische Physik,
Universität Tübingen, Auf der Morgenstelle 14,
D-7400 Tübingen, Fed. Rep. Germany.

Abstract

The convergence of the expansion for the effective interaction is studied considering as examples the shell model for the nuclei ^{18}O and ^{18}F. In this work the effective interaction is computed through third order in the Brueckner G matrix using both a harmonic-oscillator (HO) basis and a Brueckner-Hartree-Fock (BHF) basis. We report significant differences in the convergence behavior of the effective interaction in these two cases. Our results indicate that the choice of the BHF single-particle potential facilitates the convergence of the effective interaction in low-orders of the expansion, whereas the HO results exhibit a non-convergent behavior. The implications for the HO approach are discussed. All calculations have been performed considering a modern version of the Bonn one-boson-exchange potential for the nucleon-nucleon interaction.

The successful reproduction of many nuclear properties by Wildenthal, Brown and collaborators [1] using empirically derived shell-model matrix elements, has given a renewed motivation for attempts to determine these matrix elements in a microscopic theory from a realistic nucleon-nucleon (NN) interaction. Such attempts may also provide very useful informations on the differences between models for realistic NN interactions, which have recently been developed [2,3], to those which have been existing already for some years. The convergence of the different attempts [4] to obtain a perturbative expansion for the effective interaction, however, is still an open question.

After the very promising investigations by Kuo and Brown [5], where the effective interaction was approximated by a bare G-matrix plus the core-polarization term, the inclusion of higher-order terms was met with only partial success. Barrett and Kirson [6] suggested that the perturbation expansion in terms of the G-matrix did not converge. The abovementioned results where all obtained by using phenomenological NN potentials. Thus, recently Hjorth-Jensen and Osnes readdressed the convergence problem of the effective interaction in a shell-model calculation for mass-18 nuclei [7], using modern NN potentials.

However, still evidence for a non-convergent behavior was found in certain low-lying states, and the qualitative behavior of H_{eff} through third order was similar to that obtained with the phenomenological potentials. H_{eff} in [7] was computed using a harmonic-oscillator (HO) basis, assuming that these single-particle wavefunctions are sufficiently close to the self-consistent wavefunctions resulting from a Brueckner-Hartree-Fock (BHF) calculation. With this assumption a certain set of diagrams (some examples are displayed in figure 1) can be ignored and one hopes that the convergence of the expansion is improved if all those diagrams are taken into account via the BHF choice for the wavefunction.

This hope has been supported by Anastasio et al. [8], who studied a three-level Lipkin model. In this model calculation, an excellent agreement with the exact solution was obtained when the Hartree-Fock choice was made. The results indicated that the Hartree-Fock procedure facilitated the convergence of the linked-valence H_{eff} expansion [9]. Other studies, employing more realistic Hamiltonians, gave rize to the conclusion that certain classes of higher order terms are made small in the BHF basis [10,11,12].

The advantage of the BHF basis as compared to a HO basis, which is chosen in a more or less arbitrary way, can also be seen from a different point of view. Solving the BHF equations for the core nucleus (^{16}O in our example) one obtains an approximation for the wavefunction of the groundstate which is optimized with respect to particle-hole excitations to be admixed by the G matrix. Therefore one can expect that also the admixture of three-particle one-hole components to the configurations of 2 valence nucleons outside the core will be small.

We have calculated H_{eff} using version A of the Bonn potential as defined in

table A.1 of [2]. This potential has been fitted to describe the NN scattering phase shifts considering the exchange of π, ρ, δ, σ, η , and ω-mesons in the Blanckenbecler-Sugar reduction of the Bethe-Salpeter equation. This potential exhibits a very weak tensor force (the d-state probability in the deuteron is predicted to be $P_D \approx 4.4\%$), consistent with the analysis of πN data and indicated from empirical deductions of shell model matrix elements as well [13].

For nuclear structure physics, a weak tensor force has several important consequences, amongst these is the possibility to treat light and medium-heavy nuclei in the framework of two-body forces only [3]. Also, it was found by Sommerman et al. [14] that the core-polarization diagram could be approximated quite well by including excitations of $2\hbar\omega$ only in oscillator energy. For phenomenological potentials one had to include excitations up to $12\hbar\omega$ to achieve a reasonable convergence, a fact which was ascribed to the much stronger tensor force of these potentials. Clearly, a weak tensor force opens up for the possibility of calculating higher-order diagrams in an expedient and reliable way.

The Bethe-Goldstone equation, in a form which is consistent with the Blanckenbecler-Sugar approach for the free scattering, has been solved for various starting energies [15], assuming a Pauli operator which prevents scattering into intermediate particle states with a nucleon in $0s$ or $0p$ states or with both nucleons in $1s - 0d$ or $1p - 0f$ shell. The ladder terms with two particles in $1p - 0f$ shell are taken into account explicitly in the subsequent steps for evaluating H_{eff}. The effective nuclear Schrödinger equation used to define this H_{eff} is written as

$$P H_{eff} P \Psi_i = E_i P \Psi_i \tag{1}$$

and

$$H_{eff} = H_0 + V_{eff} = (T + U) + V_{eff}$$

where P is the model-space projection operator, E_i and Ψ_i are the energy and wavefunctions of the complete Hilbert space respectively, T is the kinetic energy operator and U is the single-particle potential. In this work we have chosen U to be the HO potential and the BHF potential.

Brandows [9] valence space effective interaction is then represented by a linked perturbation expansion in the G-matrix where we let

$$H_{eff}^{(i)} = H_0 + V_{eff}^{(i)} \qquad (i = 1, 2, 3) \tag{2}$$

and

$$V_{eff}^{(1)} = G \tag{3}$$

$$V_{eff}^{(2)} = G + G\frac{Q}{E_0 - H_0}G \tag{4}$$

$$V_{eff}^{(3)} = G + G\frac{Q}{E_0 - H_0}G + G\frac{Q}{E_0 - H_0}G\frac{Q}{E_0 - H_0}G \tag{5}$$

+ third-order folded terms

be the effective interaction to first, second and third order in terms of G, respectively. E_0 is the unperturbed energy of the valence space (the $1s - 0d$ shell in this work), H_0 is the unperturbed energy operator and Q is the Pauli exclusion operator. Note that V_{eff} contains one-body diagrams as well. As we calculate the eigenvalues of ^{18}O relative to ^{17}O, the one-body diagrams in the effective interaction above are then replaced by the experimental sd shell single-particle energies ($\epsilon_{s_{1/2}} - \epsilon_{d_{5/2}} = 0.87$ MeV and $\epsilon_{d_{3/2}} - \epsilon_{d_{5/2}} = 5.08$ MeV). Also, in this work we have only considered the case of a degenerate model space in both the HO and the BHF calculations, and the two-body diagrams were approximated by including excitations of $2\hbar\omega$ in oscillator energy ($\hbar\omega = 13.3$ MeV). Off-shell effects were also included in the computation of the diagrams in contrast to the abovementioned earlier calculations [7]. The latter effects reduce in general the absolute value of the diagrams included and thereby the contributions to the various orders in the perturbation expansion. The two-body diagrams included in the evaluation of V_{eff} are the same as those used in [8].

The results from the HO and BHF calculations through third order for ^{18}O and ^{18}F can be found in fig. 2 and 3, respectively. The experimental spectra are taken from the compilations of Ajzenberg-Selove [16]. In tables 1 and 2 we list the $JT = 01$ and $JT = 10$ sd two-body matrix elements for various approaches to the effective interaction. We also compare our matrix elements to the empirically derived two-body matrix elements of Wildenthal [17]. The agreement between Wildenthals sd-shell matrix elements and the reported HO matrix elements is generally rather good. The largest differences occur for matrix elements involving the $d_{3/2}$ orbit, and this might be due to the difference in the $d_{3/2}$ single-particle energies. (In Wildenthal's compilations $\epsilon_{d_{3/2}} - \epsilon_{d_{5/2}} = 5.59$ MeV and $\epsilon_{s_{1/2}} - \epsilon_{d_{5/2}} = 0.78$ MeV.)

In both isospin channels, $T = 0$ and $T = 1$, the H_{eff} calculated to third order in the HO basis seems to reproduce the experimental spectra fairly well. A similar success has also been reached by Jiang et al. [18] using the same NN interaction. Note, however, that there are some differences in the assumptions made by Jiang et al. as compared to our calculation: (1) Jiang et al. use a HO basis ($\hbar\omega = 14MeV$) slightly different from the one ($\hbar\omega = 13.3$ MeV) considered here. (2) Here we include *all* two-body diagrams, folded and non-folded, through third order, whereas Jiang et al. only include diagrams through third order in the $\hat{Q}$-box expansion of Kuo and co-workers [4]. Folded diagrams are then generated by the folding of the $\hat{Q}$-boxes. (3) Folded diagrams including BHF insertions are not considered in the present expansion.

Nevertheless, one can conclude from both investigations that within the HO basis the new version of the Bonn potential seems to supply sufficient attraction to describe the binding energy of the nuclei with $A = 18$ as compared to the energy of the ^{16}O core. Calculations employing older potentials with a stronger tensor force and including the effects of folded diagrams gave too little binding. This is in

line with the observation that the potential A also yields sufficient binding in BHF calculation of nuclear matter [2] and finite nuclei [15].

However, the main interest in our present investigation is to study the differences between second and third order in the perturbation expansion. As can be seen from both figs. 2 and 3 and tables 1 and 2, third-order effects play a considerable role in the HO calculation, resulting in a gap of 1.8 MeV for ^{18}O between the ground state to second and third order in the perturbation expansion. A similar discrepancy between third and second order is also found for the lowest-lying 1^+ and 2^+ states in ^{18}F. This must be interpreted as a signal of poor convergence, if not divergence, of the perturbation expansion. A similar result has also been obtained by Skouras et al. [19], who have developed a matrix inversion technique leading to a non-perturbative renormalization of H_{eff} with respect to $2\hbar\omega$ excitations. Using the potential A one finds also there that an expansion of H_{eff} diverges for the states with (J,T) equal to (1,0) and (0,1).

This evidence of a non-convergent behavior is removed when we use the BHF basis. In this case only small differences are found between second and third order (0.07 and 0.39 MeV for the ground states of ^{18}O and ^{18}F, respectively), indicating that our choice of single-particle potential plays an essential role for the convergence behavior of H_{eff}. This supports our expectations discussed above and is also in agreement with previous observations. Using the self-consistent BHF single-particle wavefunctions, the matrix elements which are responsible for the admixture of the Q-space are reduced.

It should be pointed out, however, that there is a remarkable difference between the situation discussed e.g. in ref. [20] and the present one. In previous investigations the radius of the density distributions for the valence states was larger in the self-consistent basis than in the HO basis. Therefore one could argue that matrix-elements calculated in the BHF basis are weaker due to the short range of the NN interaction. The situation is different for the present case. The BHF calculation for potential A gives a radius for the charge distribution of only 2.2 fm, which is much smaller than the empirical one (2.7 fm). Consequently we also observe BHF wavefunctions for the valence states, which are more concentrated near the origin than the corresponding HO function (see comparison in figure 4). Therefore the reduction of the matrixelements connecting P- and Q-space cannot be traced back to the short range of the interaction but are due to the self-consistent optimization.

The final results obtained in the BHF basis, however, are not in good agreement with the experimental data. In particular this is the case for the states of $J = 0$ in ^{18}O (T=1) and of $J = 1, 3$ in ^{18}F (T=0). All these combinations of J and T are candidates for intruder states, or cases in which states of the P-space are close in energy to the corresponding states in the Q-space [19]. A coupling to such intruder states would lower the energies of these states and could therefore be a mechanism to improve the calculated energies. In fact, Chakravarti et al. [21] improved the

agreement with experiment by adding phenomenological intruder-state corrections to their BHF *sd*-shell matrix elements. This could give as much as 1 MeV additional attraction to the ground state, still leaving a sizeable discrepancy with respect to the experimental binding energy.

For mass-18 nuclei we believe that, using a meson-exchange model with a weak tensor force, many-body forces may not play a significant role. The traditional two-body force picture should describe the properties of these nuclei fairly well. Also the relativistic features of the Dirac-BHF approach, necessary to reproduce the right saturation properties of nuclear matter, seem not to have a large influence. In fact, in a shell-model calculation using a one-boson-exchange (OBE) model similar to the one employed here [22], Müther et al. [23] showed that the medium effects were negligible for the low-lying spectra of light nuclei. The densities at the surface of light nuclei are actually too small to yield sizeable relativistic effects, and the relativistically calculated spectra were much similar to the non-relativistic ones.

Our investigations have demonstrated that it is necessary to employ a self-consistent basis of single-particle wavefunctions to obtain a convergent perturbation expansion for the effective interaction to be used in shell model calculations. The OBE potential A, defined in ref. [2] does not predict a very realistic density distribution for the ground state of nuclei like ^{16}O [15]. Furthermore, it also yields spectra which are too compressed compared to the experimental ones. One should therefore search for effects which can cure these problems. One possibility is obviously to account for core-deformed states via an enlarged model space, since our *sd*-shell effective interaction underestimates the coupling to these states.

References

[1] B. A. Brown, W. A. Richter, R. E. Julies and B. H. Wildenthal, Ann. Phys. **182** (1988) 192; B. A. Brown and B. H. Wildenthal, Ann. Rev. Nucl. Part. Sci. **38** (1988) 29

[2] R. Machleidt, Adv. Nucl. Phys. **19** (1989) 189

[3] R. Machleidt, K. Holinde and Ch. Elster, Phys. Rep. **149** (1987) 1

[4] T. T. S. Kuo, Proceedings of the 2nd International Spring Seminar on Nuclear Physics, Shell Model and Nuclear Structure: where do we stand?, ed. Aldo Covello, World Scientific, Singapore 1988, p. 29

[5] T. T. S. Kuo and G. E. Brown, Nucl. Phys. **A85** (1966) 40

[6] B. R. Barrett and M. W. Kirson, Nucl. Phys. **A148** (1970) 145

[7] M. Hjorth-Jensen and E. Osnes, Phys. Lett. **228B** (1989) 281; Phys. Scripta, in press

[8] M. R. Anastasio, T. T. S. Kuo, T. Engeland and E. Osnes, Nucl. Phys. **A271** (1976) 109

[9] B. H. Brandow, Rev. Mod. Phys. **39** (1967) 771

[10] J. Shurpin, H. Müther, T.T.S. Kuo and A. Faessler, Nucl. Phys. **A293** (1977) 61

[11] P.J. Ellis and H.A. Mavromatis, Nucl. Phys. **A175** (1971) 309

[12] P.J. Ellis and E. Osnes, Phys. Lett. **41B** (1972) 97

[13] W. W. Dachnick, Phys. Rep. **96** (1983) 317

[14] H. M. Sommerman, H. Müther, K. C. Tam, T. T. S. Kuo and A. Faessler, Phys. Rev. **C23** (1981) 1765

[15] K.W. Schmid, H. Müther and R. Machleidt, to be published.

[16] F. Ajzenberg-Selove, Nucl. Phys. **A475** (1987) 1

[17] B. H. Wildenthal, Prog. Part. Nucl. Phys. **11** (1984) 5

[18] M. F. Jiang, R. Machleidt, D. B. Stout and T. T. S. Kuo, Phys. Rev. **C40** (1989) 1857

[19] L.D. Skouras and H. Müther, to be published.

[20] J. Shurpin, T. T. S. Kuo and D. Strottman, Nucl. Phys. **A408** (1983) 310

[21] S. Chakravarti, P. J. Ellis, T. T. S. Kuo and E. Osnes, Phys. Lett. **109B** (1982) 141

[22] R. Machleidt and R. Brockmann, Proc. LAMPF Workshop on Dirac approaches to nuclear physics (Los Alamos, 1985), eds. J. R. Shephard, C. Y. Cheung and R. L. Boudrie, Los Alamos Conf. Report LA-10438-C (1985) p. 328

[23] H. Müther, R. Machleidt and R. Brockmann, Phys. Lett. **198B** (1987) 45

Figure 1: Examples of Hartree-Fock diagrams not included in the HO calculation.

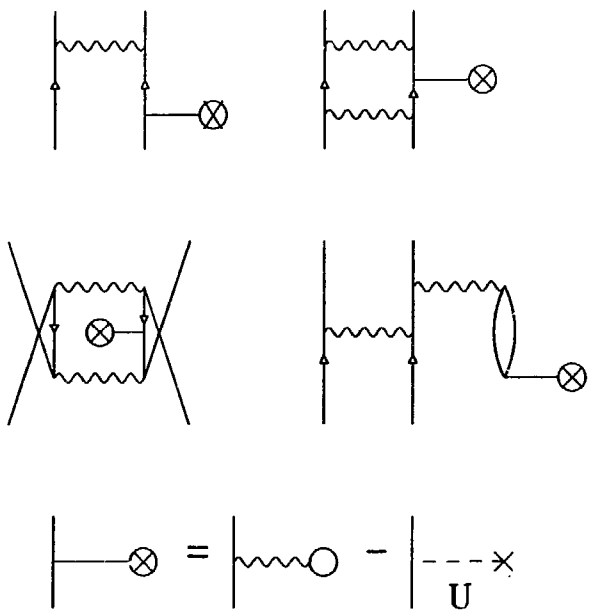
=
U

Figure 2: Theoretical and experimental low-lying positive parity spectrum for ^{18}O. $H_{eff}^{(1)}$, $H_{eff}^{(2)}$ and $H_{eff}^{(3)}$ means the effective interaction through first, second and third order respectively. All energies in MeV.

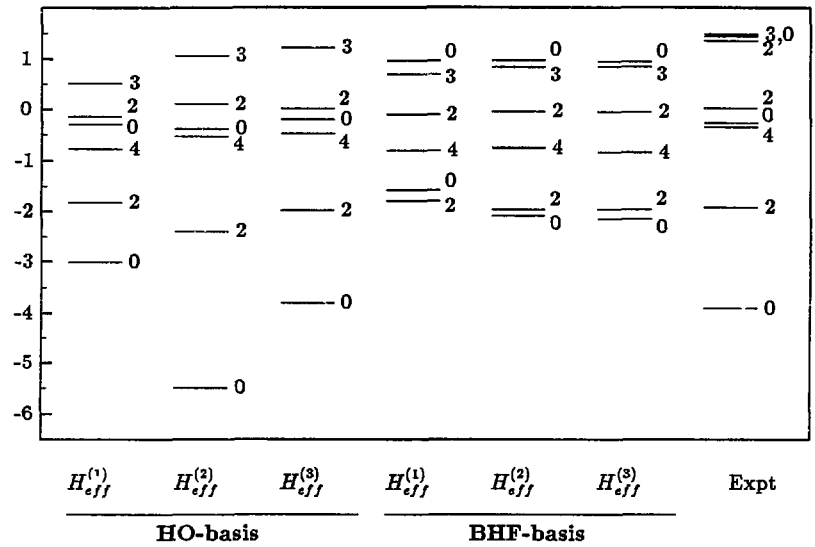
1
0
-1
-2
-3
-4
-5
-6
3
2
0
4
2
0
3
2
0
4
2
0
3
2
0
4
2
0
0
3
2
4
0
2
0
3
2
4
2
0
0
3
2
4
2
0
3,0
2
2
0
4
2
0
$H^{(1)}_{eff}$
$H^{(2)}_{eff}$
$H^{(3)}_{eff}$
$H^{(1)}_{eff}$
$H^{(2)}_{eff}$
$H^{(3)}_{eff}$
Expt
HO-basis
BHF-basis

Figure 3: Theoretical and experimental low-lying positive-parity spectrum for ^{18}F. Notation as in fig. 1.

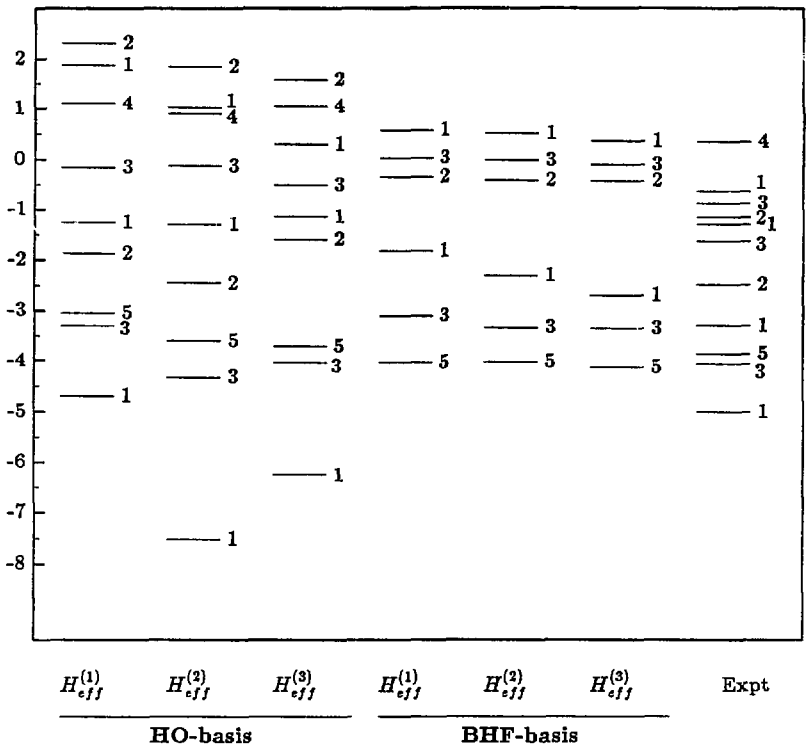
2
1
0
-1
-2
-3
-4
-5
-6
-7
-8
$H^{(1)}_{eff}$
$H^{(2)}_{eff}$
$H^{(3)}_{eff}$
$H^{(1)}_{eff}$
$H^{(2)}_{eff}$
$H^{(3)}_{eff}$
Expt
HO-basis
BHF-basis

Figure 4: Comparison of the radial wavefunction obtained in the BHF approximation for the $d_{5/2}$ state with the corresponding oscillator function.

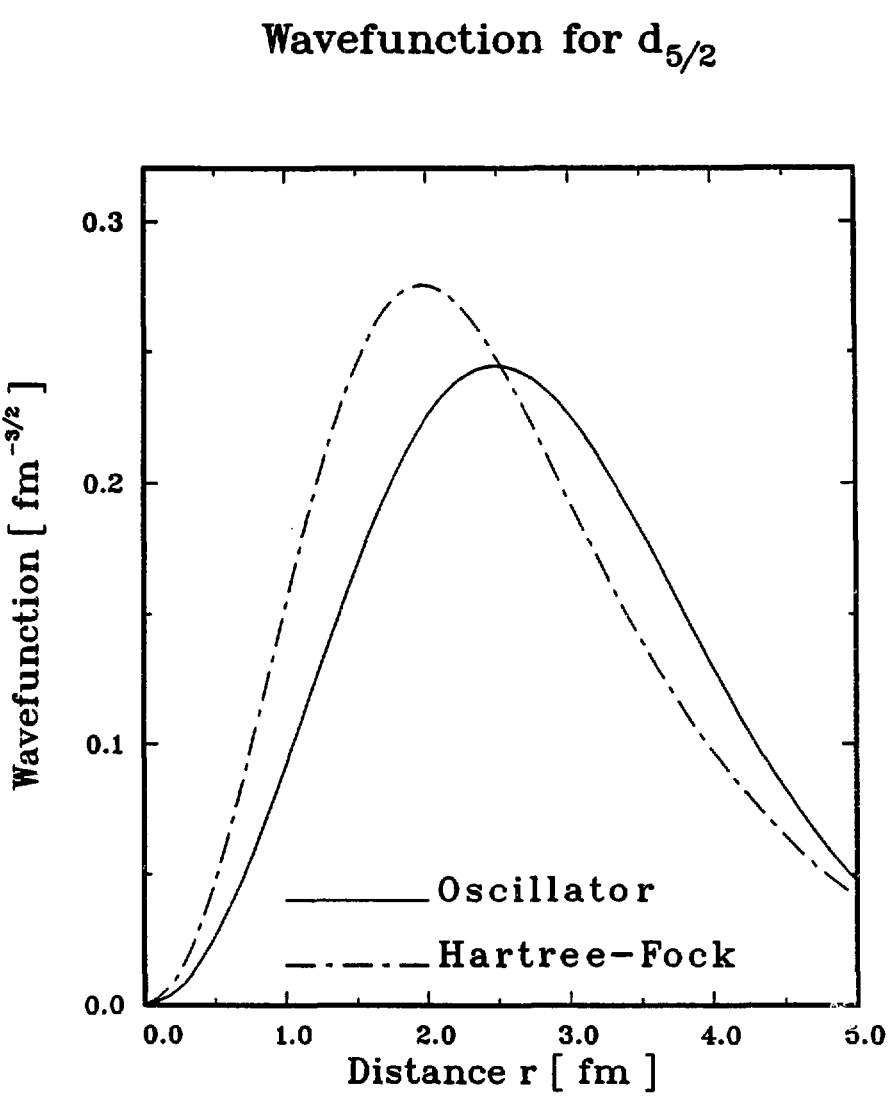
Wavefunction for $d_{5/2}$
Wavefunction [$fm^{-3/2}$]
0.3
0.2
0.1
0.0
0.0
1.0
2.0
3.0
4.0
5.0
Distance r [fm]
Oscillator
Hartree-Fock

Table 1: The $JT = 01$ sd matrix elements for various approaches to the effective interaction. In each case, the first and second rows correspond to the HO and the BHF matrix elements respectively. In the last column we list the empirically derived two-body matrix elements (TBME) of Wildenthal [17]. All entries in MeV.

				1st order	2nd order	3rd order	TBME
$d_{5/2}$	$d_{5/2}$	$d_{5/2}$	$d_{5/2}$	-1.7845	-3.6089	-2.7127	-2.8197
				-0.9985	-1.4935	-1.6474	
$d_{5/2}$	$d_{5/2}$	$d_{3/2}$	$d_{3/2}$	-3.3250	-4.4009	-2.6431	-3.1856
				-1.3384	-1.4017	-1.2261	
$d_{5/2}$	$d_{5/2}$	$s_{1/2}$	$s_{1/2}$	-0.8012	-1.3103	-1.1333	-1.3247
				-0.8044	-0.9833	-0.9634	
$d_{3/2}$	$d_{3/2}$	$d_{3/2}$	$d_{3/2}$	-0.4280	-1.4074	-1.1097	-2.1845
				-0.3852	-0.4609	-0.4175	
$d_{3/2}$	$d_{3/2}$	$s_{1/2}$	$s_{1/2}$	-0.6542	-0.9939	-0.7643	-1.0835
				-0.6191	-0.6518	-0.6148	
$s_{1/2}$	$s_{1/2}$	$s_{1/2}$	$s_{1/2}$	-2.3822	-2.6168	-2.4400	-2.1246
				-1.1477	-1.1533	-1.1449	

NOTE: The 3rd-order non-diagonal matrix elements in table 1 and 2 are the averages of the non-diagonal elements plus their hermitian conjugates, as the energy matrix is non-hermitian due to the inclusion of the third-order folded diagrams.

Table 2: The $JT = 10$ *sd* matrix elements for various approaches to the effective interaction. Notation as in table 1.

				1st order	2nd order	3rd order	TBME
$d_{5/2}$	$d_{5/2}$	$d_{5/2}$	$d_{5/2}$	-0.4051	-1.4750	-1.5313	-1.6321
				0.1235	-0.2210	-0.7899	
$d_{5/2}$	$d_{5/2}$	$d_{5/2}$	$d_{3/2}$	3.2033	4.1323	3.1030	2.5435
				2.2589	2.4172	2.3643	
$d_{5/2}$	$d_{5/2}$	$d_{3/2}$	$d_{3/2}$	2.4482	1.8511	1.4238	0.7221
				1.0811	0.9990	0.9633	
$d_{5/2}$	$d_{5/2}$	$d_{3/2}$	$s_{1/2}$	0.0730	0.2537	0.2942	1.1026
				0.2610	0.2601	0.2442	
$d_{5/2}$	$d_{5/2}$	$s_{1/2}$	$s_{1/2}$	-0.4347	-0.9759	-1.0073	-1.1756
				-0.4963	-0.6037	-0.6674	
$d_{5/2}$	$d_{3/2}$	$d_{5/2}$	$d_{3/2}$	-5.1099	-7.3911	-7.0340	-6.5058
				-1.3829	-1.8374	-2.2391	
$d_{5/2}$	$d_{3/2}$	$d_{3/2}$	$d_{3/2}$	-0.2813	-0.3302	0.1641	-0.5647
				-0.4303	-0.3805	-0.3246	
$d_{5/2}$	$d_{3/2}$	$d_{3/2}$	$s_{1/2}$	1.4663	2.0827	1.9628	1.7080
				-0.1032	0.0026	0.0482	
$d_{5/2}$	$d_{3/2}$	$s_{1/2}$	$s_{1/2}$	1.4663	2.3750	1.9328	2.1042
				1.5522	1.5884	1.5415	
$d_{3/2}$	$d_{3/2}$	$d_{3/2}$	$d_{3/2}$	-0.1523	-0.5289	-1.3992	-1.4151
				-0.1915	-0.2209	-0.2550	
$d_{3/2}$	$d_{3/2}$	$d_{3/2}$	$s_{1/2}$	-0.7822	-0.8023	-0.7603	-0.3983
				-0.5529	-0.5776	-0.5519	
$d_{3/2}$	$d_{3/2}$	$s_{1/2}$	$s_{1/2}$	-0.3639	-0.0657	0.1473	0.0275
				-0.0121	0.0172	0.0265	
$d_{3/2}$	$s_{1/2}$	$d_{3/2}$	$s_{1/2}$	-2.6893	-3.1119	-3.4883	-4.2930
				-1.6851	-1.7765	-1.8322	
$d_{3/2}$	$s_{1/2}$	$s_{1/2}$	$s_{1/2}$	0.0450	-0.4816	-0.5661	-1.2501
				0.2728	0.2045	0.1533	
$s_{1/2}$	$s_{1/2}$	$s_{1/2}$	$s_{1/2}$	-3.5535	-3.9087	-3.8488	-3.2628
				-1.5773	-1.6630	-1.7307	

FYSISK INSTITUTTS 8 FORSKNINGS-GRUPPER	DEPARTMENT OF PHYSICS RESEARCH SECTIONS
Allmennfysikk og didaktikk	General Physics
Biofysikk	Biophysics
Elektronikk	Electronics
Elementærpartikkel-fysikk	Experimental Elementary Particle physics
Faste stoffers fysikk	Condensed Matter physics
Kjernefysikk	Nuclear physics
Plasma-, molekylar- og kosmisk fysikk	Plasma-, Molecular and Cosmic physics
Teoretisk fysikk	Theoretical physics

ISBN -